MYELOID NEOPLASIA

SGN-CD33A: a novel CD33-targeting antibody–drug conjugate using a pyrrolobenzodiazepine dimer is active in models of drug-resistant AML

May S. Kung Sutherland,[1] Roland B. Walter,[2,3] Scott C. Jeffrey,[1] Patrick J. Burke,[1] Changpu Yu,[1] Heather Kostner,[1] Ivan Stone,[1] Maureen C. Ryan,[1] Django Sussman,[1] Robert P. Lyon,[1] Weiping Zeng,[1] Kimberly H. Harrington,[2] Kerry Klussman,[1] Lori Westendorf,[1] David Meyer,[1] Irwin D. Bernstein,[2,4] Peter D. Senter,[1] Dennis R. Benjamin,[1] Jonathan G. Drachman,[1] and Julie A. McEarchern[1]

[1]Department of Research & Translational Medicine, Seattle Genetics, Inc., Bothell, WA; [2]Clinical Research Division, Fred Hutchinson Cancer Research Center, Seattle, WA; and [3]Division of Hematology/Department of Medicine, and [4]Department of Pediatrics, University of Washington, Seattle, WA

Key Points

- SGN-CD33A is a novel antibody-drug conjugate, consisting of an engineered anti-CD33 mAb conjugated to a potent DNA cross-linking cytotoxin.
- SGN-CD33A is highly active in a broad panel of preclinical AML models and, in contrast to GO, is active despite MDR or poor-risk cytogenetics.

Outcomes in acute myeloid leukemia (AML) remain unsatisfactory, and novel treatments are urgently needed. One strategy explores antibodies and their drug conjugates, particularly those targeting CD33. Emerging data with gemtuzumab ozogamicin (GO) demonstrate target validity and activity in some patients with AML, but efficacy is limited by heterogeneous drug conjugation, linker instability, and a high incidence of multidrug resistance. We describe here the development of SGN-CD33A, a humanized anti-CD33 antibody with engineered cysteines conjugated to a highly potent, synthetic DNA cross-linking pyrrolobenzodiazepine dimer via a protease-cleavable linker. The use of engineered cysteine residues at the sites of drug linker attachment results in a drug loading of approximately 2 pyrrolobenzodiazepine dimers per antibody. In preclinical testing, SGN-CD33A is more potent than GO against a panel of AML cell lines and primary AML cells in vitro and in xenotransplantation studies in mice. Unlike GO, antileukemic activity is observed with SGN-CD33A in AML models with the multidrug-resistant phenotype. Mechanistic studies indicate that the cytotoxic effects of SGN-CD33A involve DNA damage with ensuing cell cycle arrest and apoptotic cell death. Together, these data suggest that SGN-CD33A has CD33-directed antitumor activity and support clinical testing of this novel therapeutic in patients with AML. (*Blood*. 2013;122(8):1455-1463)

Introduction

Acute myeloid leukemia (AML) remains a challenge in hematologic oncology, with an estimated 13 780 new cases and 10 200 deaths in the last year in the United States alone.[1] Outcomes are particularly poor in older individuals because of a lower tolerance for the intensive chemotherapy required to achieve morphologic remission and because of a higher prevalence of chemoresistance (multidrug resistance [MDR]), primarily mediated through the ATP-binding cassette superfamily of proteins such as P-glycoprotein (ATP-binding cassette B1).[2-6] Thus, there is ongoing need for new, efficacious, and better-tolerated therapeutics for patients with AML.

In addition to systemic chemotherapy, the use of monoclonal antibodies (mAbs), including those conjugated to potent cytotoxic agents, has been a focus of preclinical and clinical investigation during the past 15 years. The majority of those antibodies developed to date target the sialic acid–binding sialoadhesin receptor family member CD33 (sialic acid–binding sialoadhesin receptor 3), which is expressed on malignant cells in the vast majority of patients with AML.[7-10] Although unconjugated anti-CD33 antibodies were found to be largely ineffective in patients with AML,[11,12] encouraging results were obtained with gemtuzumab ozogamicin (GO), a CD33-targeting antibody–drug conjugate (ADC) employing calicheamicin as the toxic moiety.[9,10] Specifically, GO has single-agent activity in a subset of patients with relapsed AML,[13,14] and more important, it has recently been shown to improve survival in some patients with newly diagnosed AML and in patients with more favorable disease characteristics if added to standard induction chemotherapy.[9,10,15-18] Although concerns about increased deaths associated with GO and the lack of overall survival benefit when combined with standard induction therapy in a phase 3 trial with de novo patients with AML led to voluntary market withdrawal of the drug in 2010, these new findings provide the confirmation that CD33 is an important target in AML.[9,10]

Here we report the preclinical development and characterization of a novel ADC, SGN-CD33A, which consists of an anti-CD33

Submitted March 18, 2013; accepted June 2, 2013. Prepublished online as *Blood* First Edition paper, June 14, 2013; DOI 10.1182/blood-2013-03-491506.

Partially presented as a poster at the 54th annual meeting of the American Society of Hematology, Atlanta, GA, December 10, 2012.

The online version of this article contains a data supplement.

There is an Inside *Blood* commentary on this article in this issue.

The publication costs of this article were defrayed in part by page charge payment. Therefore, and solely to indicate this fact, this article is hereby marked "advertisement" in accordance with 18 USC section 1734.

mAb conjugated to a novel synthetic pyrrolobenzodiazepine (PBD) dimer structurally related to anthramycin isolated from *Streptomyces refuineus*. Molecules in the PBD family cause cell death by crosslinking DNA and interrupting cell division and are being explored clinically for the treatment of human cancer.[19-21] Our findings demonstrate that SGN-CD33A has robust activity in vitro against a broad panel of AML cell lines and primary patient samples, as well as in vivo using preclinical AML models, including those in which GO had minimal effect.

Materials and methods

h2H12ec mAb and synthesis of SGN-CD33A

Antibodies directed against human CD33 were generated in Balb/c mice by immunization with a recombinant human CD33-Fc fusion protein encompassing the extracellular domain (Asp18-His259). A murine clone, m2H12, was selected on the basis of its binding affinity to human and nonhuman primate CD33 and its ability to deliver cytotoxic drugs in cytotoxicity assays. The m2H12 antibody was humanized by aligning the murine VH and VL sequences to functional human germline sequences. Constructs were made on the basis of framework homology and canonical structure. Humanized/chimeric hybrid variants were screened for binding to CD33-positive cell lines and selected on the basis of binding properties that matched closely those of m2H12. The final antibody, h2H12, was engineered to contain a cysteine at position 239 on the heavy chain (IgG_1, S239C [Ser–Cys] mutation) for site-specific drug attachment that enabled the development of a well-defined, monomeric product. Subsequently, this h2H12ec antibody was linked to the PBD dimer (SGD-1882) via a maleimidocaproyl-valine-alanine drug linker, as described previously.[22]

Human AML cell lines

Human AML cell lines were obtained from the American Type Culture Collection (Manassas, VA) or Deutsche Sammlung von Mikroorganismen und Zellkulturen (Braunschweig, Germany). The cells were grown according to the supplier's instructions, using media and heat-inactivated fetal bovine sera from LifeTech (Carlsbad, CA). The presence of drug transporter activity was functionally determined via efflux of the substrate dye, rhodamine 123 (supplemental Figure 1, available on the *Blood* Web site).[23]

Primary patient samples

Eighteen diagnostic specimens from patients with newly diagnosed AML and more than 40% blasts in the bone marrow were obtained from repositories of the Children's Oncology Group and Fred Hutchinson Cancer Research Center (FHCRC; supplemental Table 1). Samples were immunophenotyped with fluorescent-labeled antibodies against CD33, CD34, and CD38 (BD Biosciences, San Jose, CA). The activities of P-glycoprotein, multidrug resistance protein, and breast cancer resistance protein were determined using a commercial flow cytometric kit (eFLUXX-ID; ENZO Life Sciences, Plymouth Meeting, PA; supplemental Figure 1). Human specimen research was approved by the Institutional Review Board at FHCRC.

In vitro saturation and internalization studies

For binding studies, AML cell lines (HL-60 and HEL 92.1.7) and HEK-293F cells engineered to express either full-length human or cynomolgus CD33 were incubated with increasing concentrations of AlexaFluor (AF) 647-labeled anti-CD33 mAb (0.85 pM to 50 nM) on ice for 30 minutes. Cells were pelleted by centrifugation, washed, and resuspended in PBS + 1% bovine serum albumin before flow cytometric analysis. The fluorescent readout was used to determine percentage bound and to calculate apparent Kd. A similar method was used to conduct the competition-binding studies except that the cells were incubated for 1 hour with a fixed amount of labeled antibody (1 nM AF647-labeled m2H12) because of the addition of increasing concentrations (30 pM to 600 nM) of unlabeled antibody. The fluorescent readout was used to determine percentage bound AF647-m2H12 mAb. The EC_{50} was extrapolated by fitting the data to a sigmoidal dose–response curve with variable slope, using Prism (GraphPad, San Diego, CA). For internalization and trafficking studies, human HNT-34 AML cells were first kept on ice in the presence of 100 ng/mL SGN-CD33A to facilitate binding before further incubation for varying times at 37°C in a tissue culture incubator to track the disappearance of the ADC-CD33 complex from the cell surface. The cells were then washed with cold PBS to remove unbound ADC and were allowed to adhere to poly-*d*-lysine coated slides (BD Biosciences) before fixation/permeabilization with Cytofix/Cytoperm (BD Biosciences). Bound ADC was detected with AF488-labeled goat anti-human IgG (Molecular Probes, Eugene, OR). Lysosomal compartments were visualized with AF647-labeled LAMP-1 antibody (mouse CD107; BD Biosciences), whereas nuclei were stained with DAPI (4′,6-diamidino-2-phenylindole; BD Biosciences). Fluorescence images were acquired with a Carl Zeiss Axiovert 200M microscope.

Determination of in vitro drug-induced cytotoxicity

For in vitro cytotoxicity assays with AML cell lines, cells were incubated with ADC in RPMI-1640 media supplemented with 10% heat-inactivated human serum (Gemini Bio Products, West Sacramento, CA) for 96 hours. Cell viability was measured with CelltiterGlo (Promega, Madison, WI), and luminescence was determined using an Envision Xcite multiplate reader (PerkinElmer, Waltham, MA). In some studies, cells were first treated with ADC or unconjugated SGD-1882 and then processed using the Annexin V-FITC Apoptosis Detection kit (EMD Millipore, Billerica, MA). Additional measurements to determine effects on DNA fragmentation (Roche Applied Sciences, Indianapolis, IN), caspase-3 activity (Promega), and mitochondrial membrane integrity (Mitocapture and Cytochrome C ELISA; ENZO Life) were performed according to the manufacturers' instructions. For in vitro cytotoxicity assays with primary patient samples, bulk cells (from 2 to 6×10^5) were incubated in Iscoves' Modified Dulbecco's medium supplemented with 20% heat-inactivated human serum and 25 ng/mL each of interleukin 3, stem cell factor, granulocyte-colony stimulating factor, and granulocyte-macrophage colony-stimulating factor (PeproTech, Rocky Hill, NJ). After 4 days, cells were stained with Annexin V and DAPI. Data were acquired on a FACSCanto flow cytometer (BD Biosciences), analyzed with FloJo software (TreeStar Inc., Ashland, OR), visualized using nonlinear regression analysis (GraphPad), and reported as IC_{50}, the concentration of compound needed to yield a 50% reduction in viability compared with vehicle-treated cells (control = 100%).

Cell cycle analyses

For cell cycle analysis, AML cells were labeled for 30 minutes with bromodeoxyuridine (BrdU; BD Biosciences). Nascent DNA synthesis was detected using an anti-BrdU antibody (BD Biosciences), whereas total DNA content was detected with propidium iodide by flow cytometry with a FACSCalibur instrument (BD Biosciences).

Western blotting

Cell lysates prepared with RIPA buffer (50 mM TRIS at pH 7.5 containing 1% NP-40, 150 mM NaCl, 1 mM EDTA, 1 mM EGTA, protease inhibitor cocktail [Roche] and phosphatase inhibitor sets 1 and 2 [EMD Millipore]) were run on 4% to 20% gradient TRIS-Gly mini-gels (LifeTech). After transfer, polyvinylidene difluoride membranes (LifeTech) were blotted with rabbit polyclonal antibodies recognizing p53, phospho-p53 (Ser15), cleaved poly(ADP-ribose)polymerase (Asp214), phospho-Chk1 (Ser345), phospho-Chk2 (Thr68), phospho-cdc2 (Tyr15), Bmf (G81), or β-actin (Cell Signaling Technology, Danvers, MA). To assess effects on histone 2AX (H2AX) phosphorylation, histone proteins were isolated and analyzed by Western blot according to protocols from AbCam (Cambridge, MA). Briefly, after cell lysis, histones were extracted with PBS containing 0.5% Triton-X 100 and protease inhibitors, and extracts were run on 4% to 12% BIS-TRIS NUPAGE gels (LifeTech), transferred onto nitrocellulose membranes, and blotted with anti-H2AX rabbit polyclonal (AbCam) and anti-phospho-H2AX mouse monoclonal (EMD Millipore) antibodies. After washing, blots were incubated with appropriate HRP-conjugated secondary antibodies (Jackson Immunoresearch, West Grove, PA), and immunoreactive signals

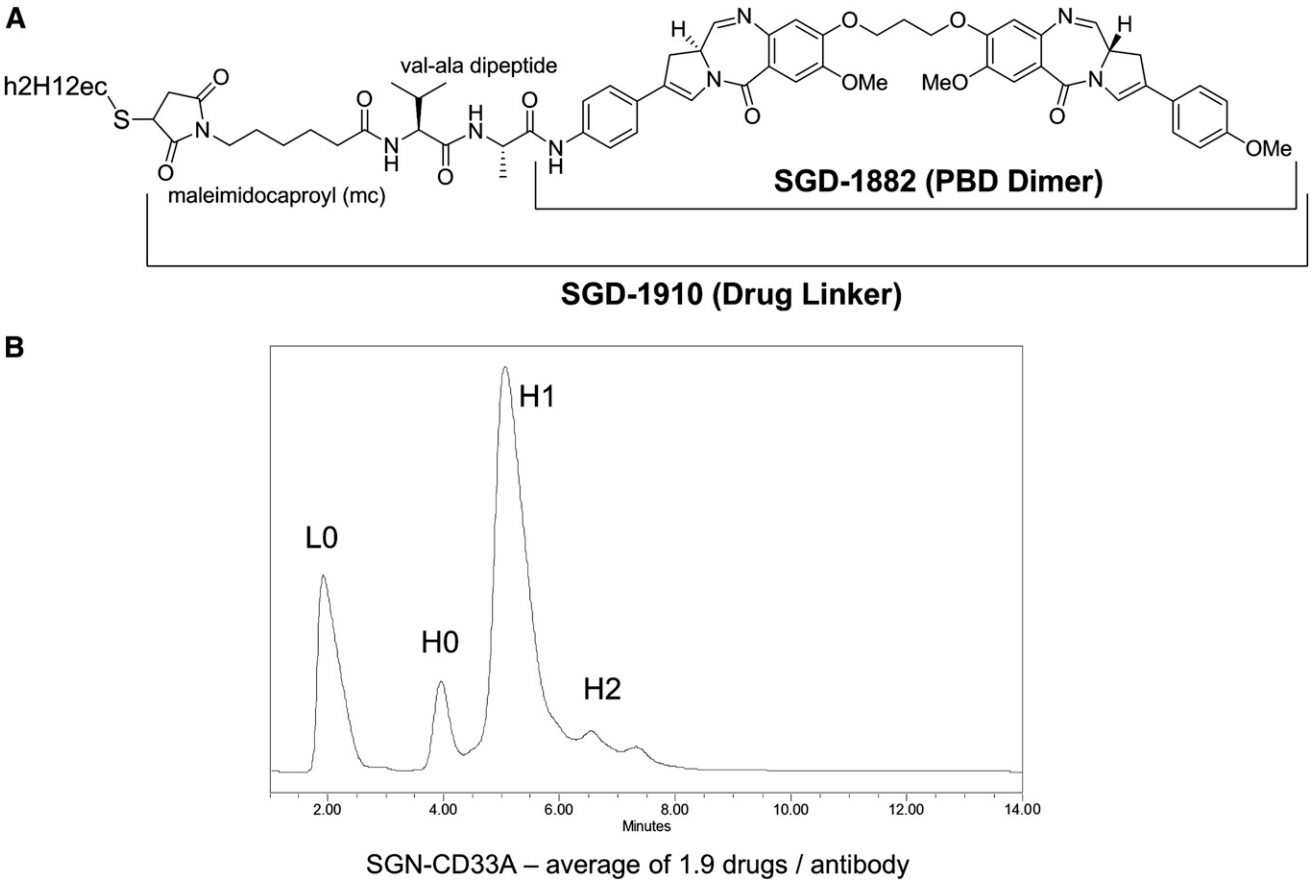

Figure 1. Characteristics of SGN-CD33A. (A) Structure of SGN-CD33A. (B) Homogeneity of drug loading on SGN-CD33A as determined by reverse-phase chromatography (PLRP). The ADC was treated with sodium cyanoborohydride for 1 hour at room temperature followed by a 15-minute incubation with 10 mM dithiothreitol. Peak areas were integrated for the unloaded (L0, H0) and drug-loaded (H1, H2) antibody chains and were used to calculate the average drug-load per antibody. H, heavy chain; L, light chain.

were visualized with chemiluminescent reagents (Supersignal West Pico; ThermoScientific, Rockford, IL).

Assessment of SGN-CD33A activity against in vivo models of human AML

All animal experiments were conducted in a facility accredited by the Association for Assessment of Laboratory Animal Care under Institutional Animal Care and Use Committee guidelines and appropriate animal research approval. Localized models of AML were established in female C.B-17 SCID mice (Harlan, Indianapolis, IN) by implanting 5×10^6 cells (HEL 92.1.7, TF1-α, and HL-60) subcutaneously in the flank. Tumor growth in the localized models was monitored throughout the course of the study with bilateral vernier caliper measurements, and mean tumor volumes were calculated using the equation ($0.5 \times$ [length $\times$ width^2]). When tumors reached approximately 100 mm^3, mice were randomly assigned to receive SGN-CD33A, GO, a control nonbinding ADC, or unconjugated h2H12ec intraperitoneally. SGD-1882, when administered, was given intravenously. For the disseminated model of disease, 5×10^6 TF1-α cells were injected intravenously into the lateral tail vein. Animals were observed and euthanized for evidence of significant progressive disease (eg, hind limb paralysis, weight loss of more than 15%); more than 90% of the untreated mice required euthanizing within 45 to 60 days after tumor cell administration as a result of progressive AML. Treatment with test compounds occurred 7 days after injection, when tumor cells were detectable in the circulation and bone marrow. For the primary AML xenograft model, NOD/SCID/*IL-2Rg*^{null} mice (NSG; The Jackson Laboratory, Bar Harbor, ME) were irradiated with 1 Gy 1 day before intravenous injection of 7×10^5 primary leukemia cells from a patient with relapsed AML (06227; AllCells, Emeryville, CA). Disease burden in the blood and bone marrow was monitored periodically by flow cytometric staining of human CD45$^+$/CD33$^+$ cells, and treatment was initiated when tumor burden in the bone marrow approached 80% (typically around 80 days postimplant). To monitor treatment effects, small amounts of bone marrow were obtained from the femoral notch region between the epicondyles from mice under anesthesia and analyzed by flow cytometry. Data were plotted and analyzed using the logarithmic rank (Mantel Cox) test (GraphPad).

Results

Basic characteristics of SGN-CD33A

SGN-CD33A was generated by conjugating a PBD dimer (SGD-1882) via the maleimidocaproyl-valine-alanine dipeptide linker to engineered cysteine residues (S239C) on h2H12ec (Figure 1A). The latter was introduced to facilitate precise loading of the mAb; indeed,

Table 1. Saturation and competition binding of unconjugated anti-CD33 antibodies and SGN-CD33A on human CD33$^+$ cell lines

Antibody	Saturation binding, nM		Competition binding, nM
	HL-60	HEL 92.1.7	293F-huCD33
m2H12	NT	NT	7
h2H12	NT	NT	5
h2H12ec	1.3	0.6	5.6
SGN-CD33A	1.2	0.5	NT

Saturation binding studies on HL-60 and HEL 92.1.7 cell lines were performed in the presence of 10% human serum. Detection was done with anti-human κ light chain FITC-labeled secondary antibody. Competition binding studies were performed with 6 nM AF488-labeled m2H12 antibody on 293F cells stably expressing 200 000 copies of full-length human CD33. NT, not tested.

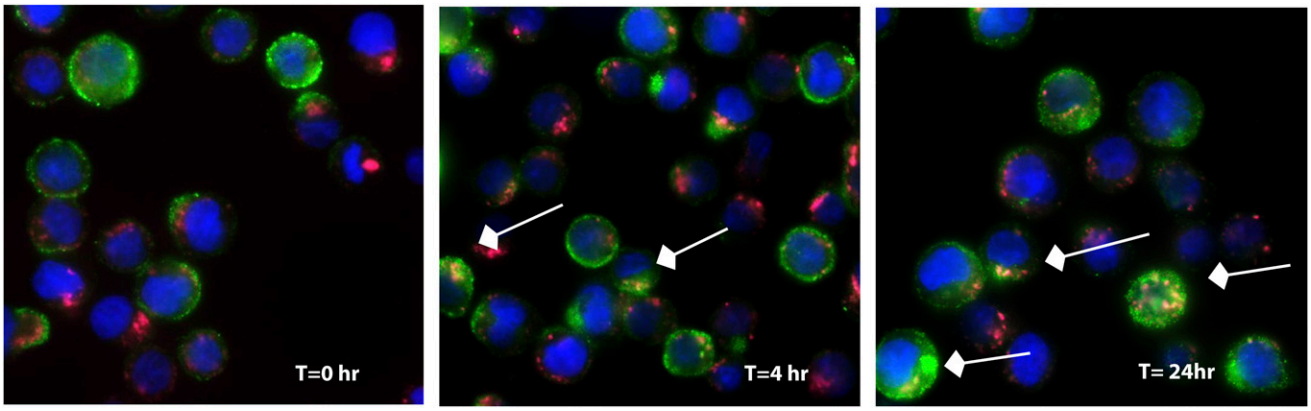

Figure 2. Internalization and trafficking of SGN-CD33A. HNT-34 cells were labeled with SGN-CD33A and incubated for up to 24 hours at 37°C. At the indicated times, cells were fixed, permeabilized, and SGN-CD33A visualized using a fluorescently labeled secondary antibody (green). To study cellular localization of SGN-CD33A, cells were also stained with anti-Lamp1 antibody (red) and DAPI (blue) to mark lysosomes and nuclei, respectively. Arrows indicate examples of colocalized signal (yellow) observed in the merged images. Magnification, 630×, oil immersion.

as determined by reverse-phase liquid chromatography, drug loading was very homogeneous, averaging 1.9 PBD moieties per antibody (Figure 1B). Proteolytic cleavage of the peptide linker is required to release SGD-1882 from the ADC (data not shown). The relative binding affinity of the antibody and ADC for CD33 was determined using saturation binding and competition binding studies. As summarized in Table 1, the K_D values for m2H12, h2H12, h2H12ec, and SGN-CD33A, determined for human CD33 expressed as an endogenous protein in 2 AML cell lines (HL-60 and HEL 92.1.7) or as a recombinant protein in HEK293F-transfected cells, were comparable. As demonstrated with HNT-34 AML cells (Figure 2) and other AML cell lines (not shown), binding of SGN-CD33A to CD33 on the cell surface resulted in internalization of the ADC-CD33 complex and colocalization with the lysosomal compartment within hours, confirming cellular uptake after target recognition.

In vitro cytotoxicity of SGN-CD33A against CD33+ AML cells

The antitumor activity of SGN-CD33A was first assessed in a panel of $CD33^+$ AML cell lines. As shown in Table 2, SGN-CD33A was highly active against all 12 tested cell lines regardless of MDR or p53 status, with a mean IC_{50} of 22 ng/mL. In comparison, GO exhibited activity against only 8 of these cell lines with a mean IC_{50} of 59 ng/mL. Notably, SGN-CD33A was active against all 4 MDR^+ cell lines (mean IC_{50}, 30 ng/mL), whereas GO demonstrated moderate activity in only 1 of the 4 cell lines (IC_{50}, 227 ng/mL for the responsive line and $IC_{50} > 1000$ ng/mL for the others). In contrast, both ADCs were inactive against 3 non-AML cell lines (Table 2). The effects of SGN-CD33A were then investigated in diagnostic specimens from patients with AML. As summarized in Table 3, SGN-CD33A was found to be active against 15 of 18 primary AML samples, with higher potency (mean IC_{50} for responsive samples, 8 ng/mL) than GO, which showed activity in 10 of 18 AML samples (mean IC_{50} for responsive samples, 27 ng/mL). Of note, SGN-CD33A activity was seen in specimens across the entire cytogenetic risk spectrum (ie, unfavorable, intermediate, and favorable), whereas the activity of GO was reduced or absent in MDR^+ samples or in patients with unfavorable cytogenetics.

Although no significant correlation was found between ADC activity and levels of CD33, the activity of both ADCs was reduced

Table 2. Cytotoxicity of SGN-CD33A and GO in AML cell lines

Cell line	Cell type	CD33 receptor copy number	MDR status	Flt3 mutation*	NPM1 mutation*	p53 status*	IC_{50} (ng/mL)	
							SGN-CD33A	GO
KG-1	AML	23 000	+	No	No	Mutant	3	227
HEL 92.1.7	AML	19 000	+	No	No	Mutant	7	>1000
TF1-α	AML	17 000	+	No	NT	Wild-type + Mutant	49	>1000
TF-1	AML	6000	+	No	NT	Wild-type + Mutant	61	>1000
HNT-34	AML	22 000	+/−	No	NT	NT	26	33
U937	AML	20 000	+/−	No	NT	Mutant	22	19
MV4-11	AML	18 000	+/−	Yes	No	Wild-type	0.1	6
Shi-1	AML	25 000	—	NT	NT	Mutant	6	NT
THP-1	AML	18 000	—	No	No	Deletion	7	6
HL-60	AML	17 000	—	No	No	Deletion	1	2
SIG-M5	AML	13 000	—	No	No	Wild-type	7.5	7
SH-2	AML	7000	—	NT	NT	Mutant	68	168
Ramos	NHL	0	NT	No	No	Mutant	>1000	NT
ES-2	Ovarian Carcinoma	0	NT			Mutant	>1000	300
SKOV-3	Ovarian Carcinoma	0	NT	No	No	Deletion	>5000	>5000

$CD33^+$ AML cells and CD33-negative cell lines were incubated with increasing concentrations of SGN-CD33A or GO for 96 hours before processing with CelltiterGlo. Data are expressed as IC_{50}, the concentration of ADC required to give a 50% reduction in cell viability. CD33 receptor copy number (copies/cell) was determined by flow cytometry, using the DAKO QiFi kit. MDR, multidrug resistance; NT, not tested; +, rhodamine dye efflux more than 2-fold above background.

*http://www.sanger.ac.uk/genetics/CGP/cell lines/ and Drexler HG. DSMZ guide to Leukemic-Lymphoma Cell Lines (http://www.dsmz.de/research/human-and-animal-cell-lines/guide-to-leukemia-lymphoma-cell-lines.html).

Table 3. Cytotoxicity of SGN-CD33A and GO in primary AML samples

Sample designation	CD33 expression (MFI)	Cytogenetic risk	MDR status	IC_{50} (ng/mL)	
				SGN-CD33A	GO
SG022	10 762	Intermediate	+	0.2	0.9
SG008	5817	Favorable	+	11	80
SG003	2278	Intermediate	+	0.4	1
SG002	318	Intermediate	+	0.9	>100
SG013	299	Unfavorable	+	11	>100
SG017	216	Favorable	+	5	>100
SG004	49	Unfavorable	+	32	No Effect
SG020	20	Unfavorable	+	>100	>100
SG012	0	Intermediate	+	>100	No Effect
SG019	1850	Intermediate	+/−	0.1	0.5
SG010	1184	Favorable	+/−	23	>100
SG011	1035	Intermediate	+/−	30	100
SG009	107	Favorable	+/−	>100	80
SG001	23 223	Unfavorable	—	6	>100
SG014	6598	Unfavorable	—	0.2	0.7
SG023	3919	Intermediate	—	0.2	0.3
SG018	1355	Intermediate	—	0.2	4
SG015	353	Unfavorable	—	0.2	2

Primary AML samples were incubated with increasing concentrations of SGN-CD33A or GO for 96 hours before flow cytometric analyses of live/dead cells. Data are expressed as IC_{50}, the concentration of ADC required to give a 50% reduction in cell viability. CD33 expression on bulk tumor cells and the $CD34^+$ subset were determined by flow cytometry and expressed as MFI. The $CD34^+$ subset (data not shown) expressed CD33 if this antigen was found on the bulk tumor cells and expression levels in these 2 groups were comparable. +, fluorescence in the presence of 2 different MDR pump inhibitors more than 2-fold above background; MDR, multidrug resistance; MFI, mean fluorescence intensity.

or absent in specimens with very low expression levels of CD33, and both were inactive against 1 primary AML specimen (SG012) in which CD33 could not be detected (Table 3). SGN-CD33A also demonstrated dose-dependent and CD33-dependent effects on the formation of CFU-GM, but not erythroid colonies from normal human $CD34^+$ bone marrow progenitor cells (supplemental Figure 2). Together, these data demonstrate that SGN-CD33A selectively targets $CD33^+$ cells and displays potent cytotoxic activity toward established AML cell lines and primary AML patient samples with higher activity than GO.

Mechanism of cytotoxicity of SGN-CD33A

PBDs have previously been shown to bind to DNA and form sequence-selective DNA lesions (ie, palindromic 5′-Pu-GATC-Py-3′ interstrand cross-links), which are thought to be mainly responsible for their cytotoxic activity.[20,24] As an early marker indicating recruitment of DNA repair machinery, histone 2AX is phosphorylated at serine 139 (γH2AX) as DNA damage accumulates with such lesions.[25] As depicted in Figure 3A, treatment of MDR^+ HEL 92.1.7 AML cells for 44 to 48 hours with SGN-CD33A or the unconjugated PBD dimer (SGD-1882) resulted in dose-dependent increases in the levels of γH2AX, with levels detectable as early as 7 to 24 hours after exposure to SGD-1882 and 16 to 24 hours with the ADC (supplemental Figure 3). Furthermore, after a 2-day treatment of HEL 92.1.7 cells with SGN-CD33A or SGD-1882, marked increases in the formation of cleaved PARP, the phosphorylation of p53 and the cell cycle checkpoint kinases, Chk1 and Chk2, and in caspase-3 activity were observed (Figures 3B-C; supplemental Figure 3). The levels of these proteins increased with increasing concentrations of SGN-CD33A or PBD dimer alone compared with the levels measured in untreated cells (Figure 3B-C). In contrast, levels of Bcl-2 protein family members did not measurably change after drug treatment except for an increase in the Bcl-2-modifying factor, Bmf (Figure 3B and data not shown). Dose- and time-dependent changes in other apoptotic markers were also observed, including phosphatidylserine translocation to the outer membrane detectable by Annexin V staining, disruption of mitochondrial membrane integrity ($\Delta\Psi m$), and translocation of cytochrome c from mitochondria to the cytosol (Figure 3D-F). HEL 92.1.7 cells treated with either SGN-CD33A or SGD-1882 arrested at the G2/M phase of the cell cycle compared with untreated cells or cells treated with a nonbinding ADC (Table 4). Consistent with the overwhelming accumulation of DNA damage, fragmented DNA was detectable and apoptotic cells with condensed or fragmented nuclei were visible by microscopy within hours of treatment of AML cells with either SGN-CD33A or SGD-1882 (supplemental Figures 4 and 5). Similar dose-dependent and time-dependent effects on DNA damage responses and apoptotic mechanisms were found in p53-deficient,[26] MDR-negative HL-60 cells treated with either SGN-CD33A or SGD-1882 (supplemental Figures 3 and 6; supplemental Table 2). Together, these findings demonstrate the potent activity of both SGD-1882 and SGN-CD33A in triggering a cascade of cellular events leading to cycle arrest and apoptosis of AML cells, with pathways and outcomes that appear similar across cell lines despite differences in MDR or p53 status.

In vivo antitumor activity of SGN-CD33A

Having demonstrated potent anti-AML activity in vitro, the antitumor activity of SGN-CD33A was evaluated in several subcutaneous models (HL-60, TF1-α, and HEL 92.1.7) and 2 disseminated mouse models of AML: 1 using TF1-α cells and 1 employing a primary AML patient isolate. Complete and durable antileukemic responses were found in all mice given a single dose of 100 μg/kg SGN-CD33A or 1000 μg/kg GO in the MDR-negative HL-60 model (Figure 4A; $P = .0005$ to control groups). A lower dose of 30 μg/kg SGN-CD33A reduced tumor growth compared with the control group ($P = .0005$; Figure 4A), whereas GO had minimal activity when dosed at 100 μg/kg.

In the drug-resistant models, SGN-CD33A demonstrated similar potent antileukemic activity, with complete responses in the HEL 92.1.7 model when mice were treated with a single dose of 1000 μg/kg SGN-CD33A, and with 3 of 7 mice remaining tumor-free at the end of the study ($P < .0001$ to controls; Figure 4B). An even lower dose of SGN-CD33A (300 μg/kg) resulted in delayed tumor growth ($P < .0001$; Figure 4B), whereas GO was not active in this model even at doses as high as 1000 μg/kg (data not shown). Likewise, a single dose of 300 μg/kg SGN-CD33A resulted in complete and durable antileukemia responses in the TF1-α model, with 5 of 7 mice remaining tumor-free ($P < .0001$), whereas a lower dose of SGN-CD33A (100 μg/kg) significantly delayed tumor growth ($P < .0001$ to controls; Figure 4C). Again, GO was not active in this model in doses up to 1000 μg/kg (Figure 4C). Most important, targeted delivery of SGD-1882 (ie, via SGN-CD33A) was required to achieve complete antitumor activity, whereas no inhibition of tumor growth was observed with the unconjugated h2H12ec, an equivalent dose of free SGD-1882, or an admixture of SGD-1882 and h2H12ec (Figure 4D).

SGN-CD33A also demonstrated potent antileukemic activity in a disseminated model of the drug-resistant TF1-α, with a single dose of 100 or 1000 μg/kg significantly improving survival ($P = .002$ and $P < .0001$, respectively, compared with untreated animals;

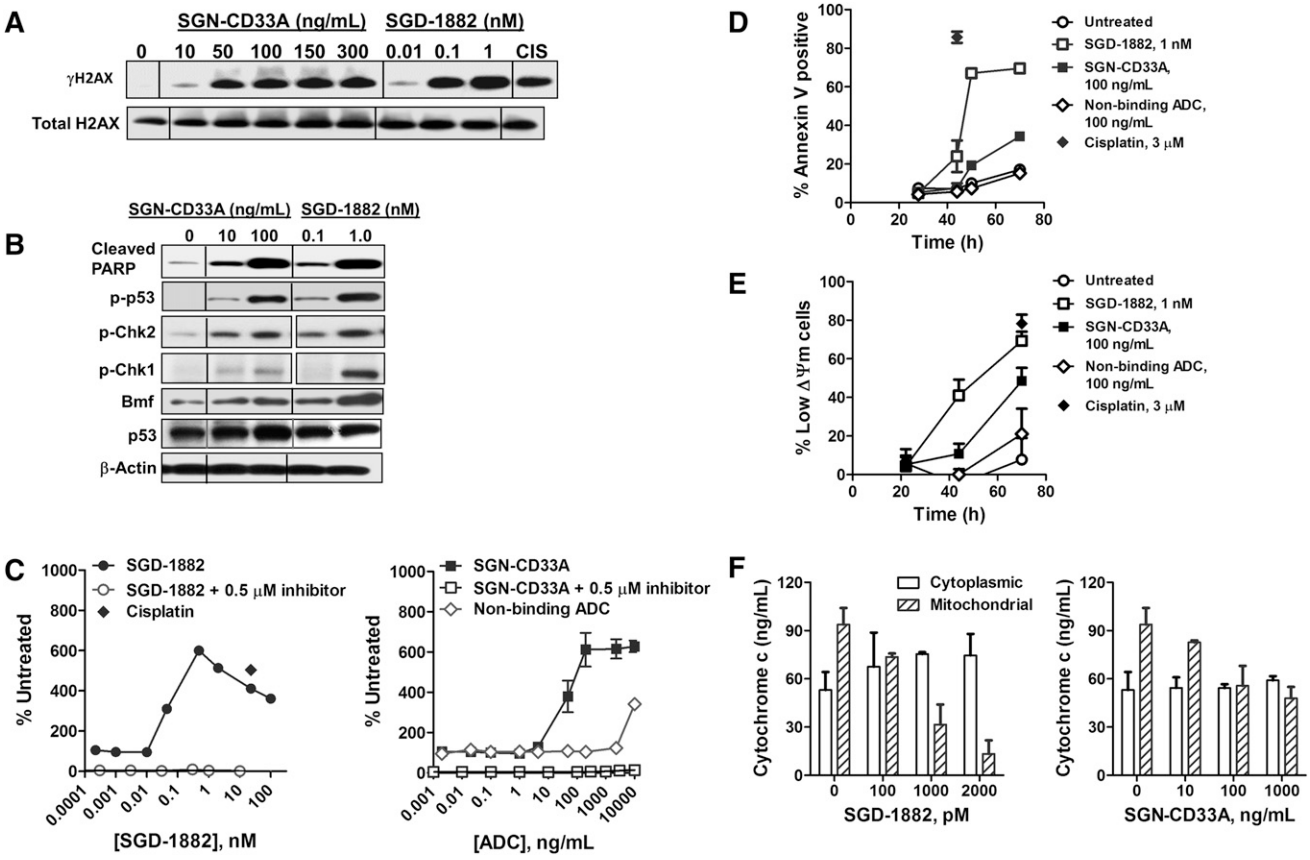

Figure 3. Mechanism of action of SGN-CD33A against MDR$^+$ HEL 92.1.7 AML cells. Cells were incubated with SGN-CD33A, SGD-1882, or a control compound (10 μM CIS, cisplatin) before processing for Western blot analyses of (A) γH2AX and (B) cleaved PARP, phospho-p53, phospho-Chk2, phospho-Chk1, and Bmf. To confirm equivalent protein loading, blots were assessed for levels of total H2AX, p53, and β-actin. Cells treated with SGN-CD33A, SGD-1882, nonbinding control ADC, and cisplatin were also evaluated for (C) caspase-3 activity, (D) annexin V staining, (E) mitochondrial membrane integrity (ΔΨm) by Mitocapture assay, and (F) cytochrome c release. Cells were processed 44 to 48 hours after initial exposure for Western blot analyses and caspase-3 activity and after 70 hours for cytochrome c release. In some experiments, cells were preincubated with a caspase inhibitor (Z-VAD-FMK, 0.5 μM) for 30 minutes before treatment with SGD-1882 or SGN-CD33A or nonbinding control. For annexin V and assay for mitochondrial integrity, cells were treated with 100 ng/mL SGN-CD33A or nonbinding control ADC, 1 nM SGD-1882, or 3 μM cisplatin. Data shown in Figure 3C-F represent mean ± SD of values from 2 to 3 experiments. One hundred nanograms per milliliter SGN-CD33A is the ADC equivalent for 1 nM SGD-1882.

Figure 4E). Three of 8 mice dosed with 1000 μg/kg ADC were alive at 120 days, whereas a nonbinding ADC or GO had no activity (Figure 4E). Finally, in the murine model established with cells from a patient with relapsed AML, in which human CD45$^+$CD33$^+$ tumor cells expanded primarily in the bone marrow, 2 doses of SGN-CD33A significantly reduced the leukemia burden between days 10 and 31 ($P < .01$ compared with untreated cohorts), with progression of the disease observed after day 45 (Figure 4F). Taken together, these data demonstrate that SGN-CD33A has marked, dose-dependent, and specific antileukemia activity in AML xenograft models that is more extensive and more potent than the activity observed with GO.

Discussion

In this report, we describe the development and preclinical testing of a novel ADC, SGN-CD33A, which consists of an engineered, humanized anti-CD33 mAb conjugated via a protease-cleavable dipeptide linker to a highly potent, synthetic DNA cross-linking PBD dimer, SGD-1882. The findings from our studies allow several general conclusions. First, the use of a mAb with engineered cysteines at the sites of drug linker attachment results in predictable, homogeneous drug loading of approximately 2 PBD dimers per ADC. Second, SGN-CD33A is highly active in a CD33-specific manner against a panel of AML cell lines and primary AML cells

Table 4. Effect of SGN-CD33A and SGD-1882 on cell cycle in HEL 92.1.7 cells

	% in phase of cell cycle		
Treatment and concentration	**G1**	**S**	**G2-M**
Untreated	50	32	12
0			
Nonbinding ADC (ng/mL)			
100	50	35	11
SGN-CD33A (ng/mL)			
1	44	36	17
10	26	36	34
100	10	22	57
SGD-1882 (nM)			
0.01	45	36	15
0.1	26	41	29
1	5	8	73

HEL 92.1.7 cells were incubated with SGN-CD33A, SGD-1882, or a nonbinding control ADC for 48 hours before BrdU incorporation and processing for flow cytometric analysis. The results shown are representative of data obtained from 3 separate experiments. Nascent DNA synthesis was detected with anti-BrdU, whereas total DNA content was determined with propidium iodide. One hundred nanograms per milliliter SGN-CD33A is the ADC equivalent of 1 nM SGD-1882.

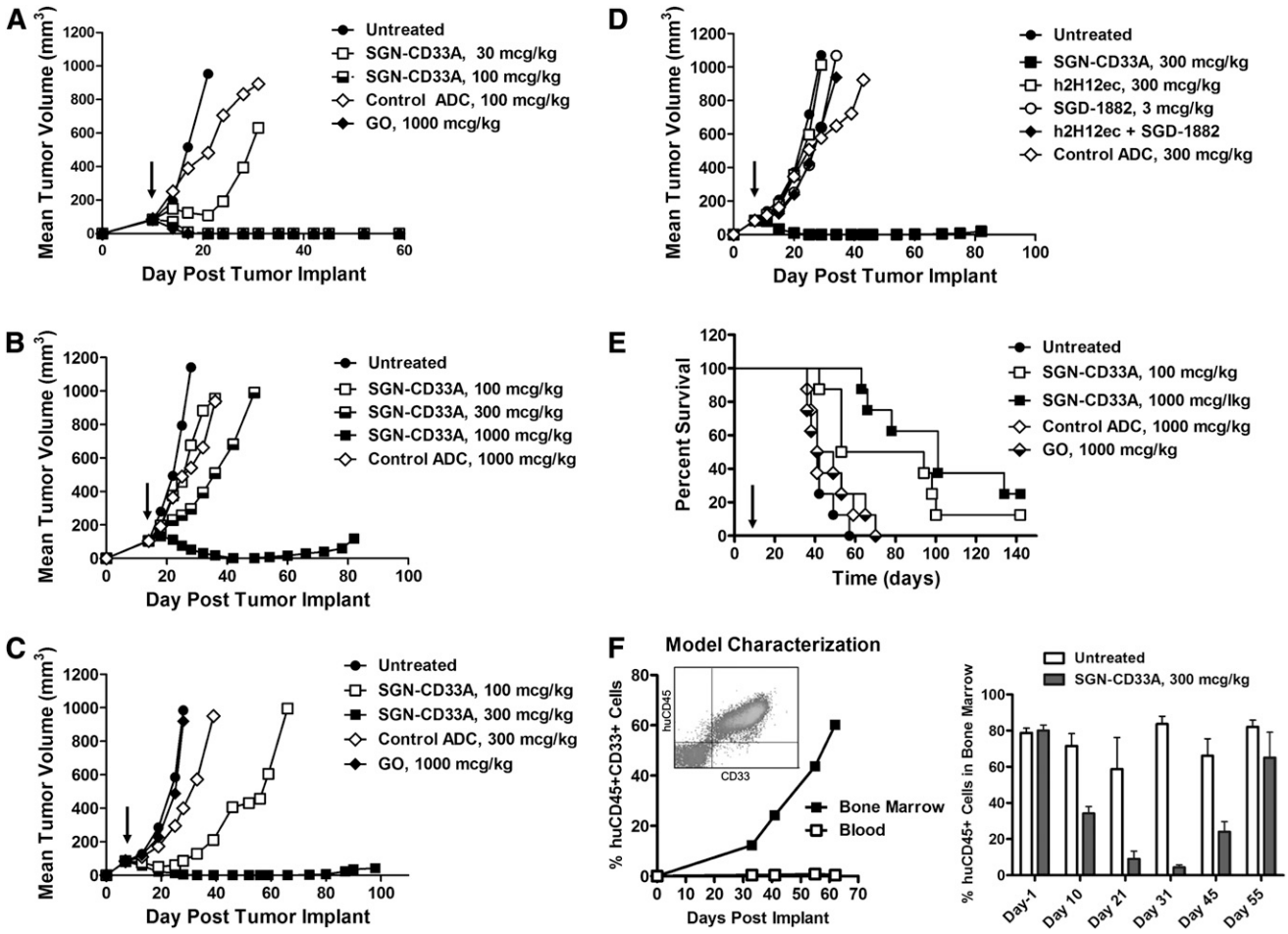

Figure 4. Single-dose antitumor activity of SGN-CD33A in MDR-negative and MDR$^+$ murine models of AML. Localized tumor models were developed in SCID mice with (A) MDR-negative HL-60 cells, (B) MDR$^+$ HEL 92.1.7 cells, or (C-D) MDR$^+$ TF1-α cells. Mice were dosed once with SGN-CD33A, nonbinding control ADC, GO, unconjugated h2H12ec, or SGD-1882 PBD dimer when tumors reached ~100 mm^3 (arrow). Antitumor activity was also assessed in disseminated models developed with (E) TF1-α and (F) cells from a patient with MDR$^+$ relapsed AML disease. Seven days after intravenous administration of TF1-α cells, SCID mice were dosed once with SGN-CD33A, nonbinding control ADC or GO (arrow). Animals were monitored and euthanized on evidence of disease. For the primary AML model, NSG mice were injected with patient isolate, and when the tumor burden in the bone marrow approached 80%, as assessed by flow cytometry (left), mice were dosed on day 0 and day 11 with 300 μg/kg SGN-CD33A (right). AML blast percentages were determined in bone marrow aspirates from live mice (day 1 and day 10; n = 12/group) and in mice terminated on days 21 to 55 (n = 3/group). SGN-CD33A treatment had no adverse effects on the health of the mice at all of the doses tested.

in vitro as well as in vivo, as evidenced by the results of the mouse xenotransplantation studies. Mechanistic studies indicate that the cytotoxic effects of this ADC involve DNA damage with resultant cell cycle arrest and apoptotic cell death. Third, potent antileukemic activity was observed in both MDR-negative and MDR$^+$ models of AML. Together, these data suggest the potential clinical utility of SGN-CD33A as a therapeutic for patients with AML and support the clinical testing of this agent.

GO has been an important paradigm for the use of antibody-based therapeutics in AML, with emerging data from well-controlled trials supporting the conclusion that CD33 is a relevant drug target for some patients with AML.[9,10] Nonetheless, several factors have been identified that have limited the clinical efficacy of GO, including heterogeneous drug loading (approximately 50% of the anti-CD33 mAb molecules are unconjugated in clinical-grade GO) and cellular efflux of the toxic GO payload, calicheamicin-γ_1, by drug transporter proteins. In fact, expression of transporter proteins has been repeatedly associated with resistance to GO both in vitro and in vivo.[27-30] This is particularly problematic, as the MDR phenotype is common in AML and has been identified as an independent factor predicting treatment failure.[5,31]

SGN-CD33A adds a significant improvement to CD33-targeted immunotherapy of AML. In particular, SGN-CD33A takes advantage of novel linker technologies, which enable the production of ADCs with uniform drug loading of antibody molecules. This is expected to considerably increase delivery and intracellular toxin uptake by targeted cells. Second, SGN-CD33A uses a toxic moiety that maintains antitumor activity despite the MDR phenotype. Indeed, SGN-CD33A was highly active against AML cell lines and primary AML cells, regardless of MDR status. Likewise, a single dose of SGN-CD33A was sufficient in reducing tumor growth and producing durable remissions in both MDR-negative and MDR$^+$ AML xenograft models, whereas GO was inactive in MDR$^+$ models. In addition, the cytotoxic activity of SGN-CD33A was not limited by cytogenetic risk (unfavorable, intermediate, or favorable). In contrast, GO was less active in samples from patients with unfavorable cytogenetics. These findings suggest that SGN-CD33A may exert significant cytotoxic effects in a broad range of AML, including those that are characterized by MDR mechanisms or poor risk cytogenetics, offering an important advantage over GO as potential therapeutic agent for the treatment of AML.

PBD dimers are a recently discovered class of potent cytotoxic agents that are thought to initiate cellular damage through DNA cross-linking that eventually leads to apoptosis and cell death.[19,20] Consistent with this presumed mechanism, SGN-CD33A or SGD-1882 induced significant increases in the levels of phosphorylated H2AX, an early DNA damage marker, and cell cycle checkpoint proteins Chk1 and Chk2. Interestingly, cytotoxic effects of these agents were observed in a wide panel of AML cell lines, regardless of p53 status, indicating that p53 was not essential for their antileukemic activity, although phosphorylation of p53 and upregulation of the proapoptotic Bcl-2 family member, Bmf, was observed in HEL 92.1.7 cells. Further studies are necessary to fully elucidate the differences in p53-dependent and p53-independent signaling events that are elicited in response to PBD dimer-induced cytotoxicity in myeloid cells.

In conclusion, our data demonstrate that SGN-CD33A is active in a broad panel of cell samples and mouse models of AML and, in contrast to GO, is active in samples despite MDR expression or poor-risk cytogenetics. Conjugation of SGD-1882 to the h2H12ec antibody imparted selectivity for $CD33^+$ cells and enhanced cytotoxic activity, an approach that may offer improved antitumor activity against emergent or residual drug resistance in AML. Given these promising preclinical findings, clinical testing of SGN-CD33A is warranted.

Acknowledgments

The authors thank Sam Blackman for reviewing the manuscript and Cyd Nourigat (Xenograft Model Core Facility, FHCRC) for sharing her expertise in conducting bone marrow harvests. The PBD dimer was licensed from Spirogen, Ltd.

Authorship

Contribution: M.S.K.S., R.B.W., and J.A.M. designed and performed experiments, analyzed and interpreted data, and wrote the paper; S.C.J., P.J.B., M.C.R., D.S., R.P.L., H.K., L.W., and K.K., designed and performed experiments and interpreted data; D.M., C.Y., I.S., W.Z., and K.H.H. performed experiments and provided figures; and D.R.B., P.D.S., I.D.B., and J.G.D. provided guidance, intellectual input, and reviewed the paper.

Conflict-of-interest disclosure: All authors are employees of Seattle Genetics, Inc., except R.B.W. and I.D.B., who are consultants, and K.H.H., who is a collaborator.

Correspondence: May Sutherland, Seattle Genetics, Inc, 21823-30th Dr SE, Bothell, WA 98021; e-mail: msutherland@seagen.com.

References

1. Siegel R, Naishadham D, Jemal A. Cancer statistics, 2012. *CA Cancer J Clin.* 2012;62(1):10-29.
2. Appelbaum FR, Gundacker H, Head DR, et al. Age and acute myeloid leukemia. *Blood.* 2006;107(9):3481-3485.
3. Döhner H, Estey EH, Amadori S, et al; European LeukemiaNet. Diagnosis and management of acute myeloid leukemia in adults: recommendations from an international expert panel, on behalf of the European LeukemiaNet. *Blood.* 2010;115(3):453-474.
4. Estey E, Döhner H. Acute myeloid leukaemia. *Lancet.* 2006;368(9550):1894-1907.
5. Leith CP, Kopecky KJ, Godwin J, et al. Acute myeloid leukemia in the elderly: assessment of multidrug resistance (MDR1) and cytogenetics distinguishes biologic subgroups with remarkably distinct responses to standard chemotherapy. A Southwest Oncology Group study. *Blood.* 1997;89(9):3323-3329.
6. Marie JP, Zittoun R, Sikic BI. Multidrug resistance (mdr1) gene expression in adult acute leukemias: correlations with treatment outcome and in vitro drug sensitivity. *Blood.* 1991;78(3):586-592.
7. Jilani I, Estey E, Huh Y, et al. Differences in CD33 intensity between various myeloid neoplasms. *Am J Clin Pathol.* 2002;118(4):560-566.
8. Legrand O, Perrot JY, Baudard M, et al. The immunophenotype of 177 adults with acute myeloid leukemia: proposal of a prognostic score. *Blood.* 2000;96(3):870-877.
9. Cowan AJ, Laszlo GS, Estey EH, Walter RB. Antibody-based therapy of acute myeloid leukemia with gemtuzumab ozogamicin. *Front Biosci.* 2013;18:1311-1334.
10. Walter RB, Appelbaum FR, Estey EH, Bernstein ID. Acute myeloid leukemia stem cells and CD33-targeted immunotherapy. *Blood.* 2012;119(26):6198-6208.
11. Jurcic JG. What happened to anti-CD33 therapy for acute myeloid leukemia? *Curr Hematol Malig Rep.* 2012;7(1):65-73.
12. Rosenblat TL, McDevitt MR, Mulford DA, et al. Sequential cytarabine and alpha-particle immunotherapy with bismuth-213-lintuzumab (HuM195) for acute myeloid leukemia. *Clin Cancer Res.* 2010;16(21):5303-5311.
13. Fenton C, Perry CM. Gemtuzumab ozogamicin: a review of its use in acute myeloid leukaemia. *Drugs.* 2005;65(16):2405-2427.
14. Sievers EL, Larson RA, Stadtmauer EA, et al; Mylotarg Study Group. Efficacy and safety of gemtuzumab ozogamicin in patients with CD33-positive acute myeloid leukemia in first relapse. *J Clin Oncol.* 2001;19(13):3244-3254.
15. Burnett AK, Russell NH, Hills RK, et al. Addition of gemtuzumab ozogamicin to induction chemotherapy improves survival in older patients with acute myeloid leukemia. *J Clin Oncol.* 2012;30(32):3924-3931.
16. Castaigne S, Pautas C, Terré C, et al; Acute Leukemia French Association. Effect of gemtuzumab ozogamicin on survival of adult patients with de-novo acute myeloid leukaemia (ALFA-0701): a randomised, open-label, phase 3 study. *Lancet.* 2012;379(9825):1508-1516.
17. Delaunay J, Recher C, Pigneux A, et al. Addition of gemtuzumab ozogamycin to chemotherapy improves event-free survival but not overall survival of AML patients with intermediate cytogenetics not eligible for allogeneic transplantation. Results of the GOELAMS AML 2006 IR study [abstract]. *Blood.* 2011;118(21):37-38.
18. Petersdorf SH, Kopecky KJ, Slovak M, et al. A phase 3 study of gemtuzumab ozogamicin during induction and postconsolidation therapy in younger patients with acute myeloid leukemia. *Blood.* 2013;121(24):4854-4860.
19. Hartley JA, Hochhauser D. Small molecule drugs - optimizing DNA damaging agent-based therapeutics. *Curr Opin Pharmacol.* 2012;12(4):398-402.
20. Smellie M, Bose DS, Thompson AS, Jenkins TC, Hartley JA, Thurston DE. Sequence-selective recognition of duplex DNA through covalent interstrand cross-linking: kinetic and molecular modeling studies with pyrrolobenzodiazepine dimers. *Biochemistry.* 2003;42(27):8232-8239.
21. Wu J, Clingen PH, Spanswick VJ, et al. gamma-H2AX Foci Formation as a Pharmacodynamic Marker of DNA Damage Produced by DNA Cross-Linking Agents: Results from 2 Phase I Clinical Trials of SJG-136 (SG2000). *Clin Cancer Res.* 2013;19(3):721-730.
22. Burke PJ, Jeffrey S, Meyer D, et al. Anti-CD70 antibody-drug conjugates containing pyrrolobenzodiazepine dimers demonstrate robust antitumor activity. In: Proceedings of the 103rd Annual Meeting of the American Association for Cancer Research; March 31-April 4, 2012; Chicago, IL. Abstract 4631.
23. Nelson EJ, Zinkin NT, Hinkle PM. Fluorescence methods to assess multidrug resistance in individual cells. *Cancer Chemother Pharmacol.* 1998;42(4):292-299.
24. Hartley JA, Spanswick VJ, Brooks N, et al. SJG-136 (NSC 694501), a novel rationally designed DNA minor groove interstrand cross-linking agent with potent and broad spectrum antitumor activity: part 1: cellular pharmacology, in vitro and initial in vivo antitumor activity. *Cancer Res.* 2004;64(18):6693-6699.
25. Rogakou EP, Nieves-Neira W, Boon C, Pommier Y, Bonner WM. Initiation of DNA fragmentation during apoptosis induces phosphorylation of H2AX histone at serine 139. *J Biol Chem.* 2000;275(13):9390-9395.
26. Han Z, Chatterjee D, He DM, et al. Evidence for a G2 checkpoint in p53-independent apoptosis induction by X-irradiation. *Mol Cell Biol.* 1995;15(11):5849-5857.

27. Matsui H, Takeshita A, Naito K, et al. Reduced effect of gemtuzumab ozogamicin (CMA-676) on P-glycoprotein and/or CD34-positive leukemia cells and its restoration by multidrug resistance modifiers. *Leukemia.* 2002;16(5): 813-819.

28. Naito K, Takeshita A, Shigeno K, et al. Calicheamicin-conjugated humanized anti-CD33 monoclonal antibody (gemtuzumab zogamicin, CMA-676) shows cytocidal effect on CD33-positive leukemia cell lines, but is inactive on P-glycoprotein-expressing sublines. *Leukemia.* 2000;14(8):1436-1443.

29. Walter RB, Raden BW, Hong TC, Flowers DA, Bernstein ID, Linenberger ML. Multidrug resistance protein attenuates gemtuzumab ozogamicin-induced cytotoxicity in acute myeloid leukemia cells. *Blood.* 2003;102(4):1466-1473.

30. Tang R, Faussat AM, Perrot JY, et al. Zosuquidar restores drug sensitivity in P-glycoprotein expressing acute myeloid leukemia (AML). *BMC Cancer.* 2008;8:51.

31. Benderra Z, Faussat AM, Sayada L, et al. MRP3, BCRP, and P-glycoprotein activities are prognostic factors in adult acute myeloid leukemia. *Clin Cancer Res.* 2005;11(21): 7764-7772.